International Journal of Automotive Technology, Vol. 21, No. 6, pp. 1339–1348 (2020)
DOI 10.1007/s12239–020–0126–4

pISSN 1229–9138/ eISSN 1976–3832

IMPACT ATTENUATOR OPTIMUM DESIGN FOR A FSAE RACING CAR BY NUMERICAL AND EXPERIMENTAL CRASH ANALYSIS

Ludovica Coppola, Bruno De Marco, Vincenzo Niola, Aleksandr Sakhnevych and Francesco Timpone*

Department of Industrial Engineering, University of Naples Federico II, Napoli 80125, Italy

(Received 11 June 2018; Revised 14 August 2019; Accepted 9 December 2019)

ABSTRACT–One of the most important requirements of the Formula SAE (Society of Automotive Engineers) race car design competition is that the car structure must guarantee a high protection level in case of frontal impacts, by preventing intrusions into the driver foot zone or dangerous deceleration levels. These functions are mainly performed by the impact attenuators, which have to guarantee a high specific energy absorption capacity (SEA) and in order to preserve vehicle performances, have to be as light weighted as possible. The aim of this study is the design of an impact attenuator, to be mounted on a Formula SAE car, which main purpose is to obtain the optimal crash energy management, maximizing the absorbed energy and optimizing the geometry. The outcome of the study highlights that the absorber structure made up of honeycomb sandwich panels (primary energy absorbers), realized by means of different aluminium alloys employing an innovative design considering particular geometrical cavities within the structure, could lead to reduce the overall weight and to achieve a more progressive deformation during the impact.

KEY WORDS : FSAE impact attenuator, Johnson Cook model, Honeycomb sandwich panel, Numerical simulation, LS-DYNA, Crash behaviour, Drop test

1. INTRODUCTION

The Formula SAE is a competition involving university students organized by the Society of Automotive Engineers (SAE) whose aim is the design and production of a racing car, evaluated during a series of tests based on its design quality and engineering efficiency.

One of the most important aspects to be evaluated is the crash safety of the vehicle.

Crashworthiness or crash safety is the capability of the vehicle structure to provide an adequate protection to its occupants from injuries in a crash event.

The safety requirements for the impact attenuator are defined by the organisers of the FSAE competition in specific rules (2017-18 Formula SAE® Rules, Access 2017).

To meet these requirements, various solutions have been designed and proposed by the different teams in the years proposing peculiar structures and employing light materials (aluminium, honeycomb, carbon, Kevlar, etc. and different combinations of these materials).

The collapse of these components should absorb the vehicle kinetic energy whilst transmitting a low load uniformly to the rest of the vehicle and maintaining an acceptable level of deformation. These impact attenuators must be made of lightweight materials, which may contribute to improving the acceleration performance of vehicles.

In this paper is developed the design of a frontal crash absorber for a formula SAE competition vehicle whose main aim is to protect the driver during a frontal crash. The criterion followed in the design is the crash energy management (CEM): the system (crash box) has to absorb the kinetic energy released during a collision and to transfer a low and possibly uniform load to the system driver-vehicle, collapsing in a controlled way, allowing simultaneously to decrease gradually the acceleration experienced by the driver to reduce the risk of injuries (the acceleration's average value has to remain below the normative limit).

This means that the impact energy has to be absorbed gradually and entirely: gradually, in order to keep a low deceleration value during the whole impact phase; entirely, in order to avoid a contact between the vehicle's frame (or the driver) and the obstacle.

So, in order to minimize the impact's damages, it is necessary to dissipate the energy deriving from the collision by absorbing it through the planned progression of the crash box deformation. To reach this objective the absorbers are often made by metallic foams or by honeycomb sandwich panels. Actually this kind of material's structure has the capability to absorb gradually high energy's levels, showing, after the impact, huge deformations, being simultaneously lightweight. The property to be lightweight helps to preserve the vehicle

**Corresponding author*: e-mail: francesco.timpone@unina.it

performances, reducing the inertia.

In literature it is possible to find different studies concerning the behaviour of honeycombs and the design and the analysis of impact attenuators.

In (Ruan *et al*., 2003) a finite element study about the in-plane dynamic crushing of honeycombs by means of ABACUS is developed with the aim to investigate the influences of honeycomb cell wall thickness and impact velocity on the mode of localised deformation and the plateau stress.

In (Wu and Jiang, 1997) the experimental results for six types of honeycomb cellular structures under quasi-static and impact loads applied in the axial direction are reported with the aim to find out the better cell size and core height for energy absorption.

In (Yamashita and Gotoh, 2005) the effect of cell shape and the foil thickness on crush behavior is investigated by numerical simulation using an explicit FEM code DYNA3D. Impact experiments using a drop-hammer apparatus whose impact velocity is 10 m/s and the corresponding quasi-static one was also performed. The numerical result, well consistent with the experimental ones, showed that the cyclic buckling mode takes place in every case and that the crush strength is higher for smaller branch angle.

In (Zhao and Gary, 1998) is studied the crush behavior of aluminum honeycombs under dynamic impact loading using a new application of the Split Hopkinson Pressure Bar (SHPB).

In (Boria, 2016) an attenuator with a shape of a truncated pyramid, made up of aluminium sandwich material with a honeycomb core separating two thin skins panels is developed. Its collapse mode and energy-absorption capability are simulated and studied by explicit finite element code and the numerical results are compared with the corresponding experimental test data. The conclusion is that the designed impact attenuator satisfies the specific homologation requirements of the FSAE, but very few details on the model and on the properties adopted for the material are provided in the paper.

In (Potabatti, 2016) is described the design of an impact attenuator with aluminium honeycomb and foam, it was tested physically under gradual load apply (quasi-static) condition, founding that it satisfied all functional requirements and design rules set up by Formula SAE.

In (Belingardi and Obradovic, 2010) is designed a crash box made of aluminum, having a truncated pyramidal structure with rounded edges, presenting opportune holes in the skins. The crash box impact is numerically simulated, but there is no experimental validation for the numerical testing.

In (Zhou *et al*., 2017) the energy absorption capacity of origami crash boxes (OCB) subjected to oblique loading is investigated compared with a conventional square tube (CST) with identical weight. The study, performed to assess the effect of geometry parameters on the energy absorption characteristics, reveals that the origami crash box is more desirable than the conventional square tube in most of the range of load angle. A bulkhead-reinforced origami crash box is proposed as a high-performance energy absorption device and an optimum structure designed.

In (D'Agostino *et al*., 2013) A software based on a genetic algorithm optimization has been developed in order to optimize the geometrical parameters of a variable-thickness crash absorber performing a numerical study on the folding of thin-walled aluminium tubes with variable-thickness in order to achieve the maximum energy absorption-to-mass ratio. The results show how the approach allows an efficient variable-thickness crash absorber to be obtained.

In (Ahmadisoleymani and Missoum, 2017) is built a risk model to predict the probability of Traumatic Brain Injury (TBI) due to car crashes, developing a multilevel framework, which includes vehicle crash Finite Element (FE) simulations with a dummy along with FE simulations of the brain using loading conditions derived from the crash simulations.

In (Ma and Lankarani, 1997) a general methodology for kineto-static analysis of multibody systems with flexible structures undergoing large motion and structural deformations is developed, rigid multibody dynamics is used to predict the gross motions and displacements at the boundaries between the relatively bulky (rigid) bodies and relatively flexible ones. A mixed boundary-condition finite-element analysis is formulated and solved at every numerical integration time to determine the corresponding reaction forces and moments at the boundaries and also the structural deformations. The analytical results obtained are compared with the experimental results from the impact sled tests. The objective is the determination of the type and probable causes of injuries that may be sustained during a crash.

In this paper the study has focused on the component geometry that could have reached the best achievable performances in terms of structural integrity, deformation capability, light weighted characteristic and compliance to FSAE safety requirements. The outcome of this study has highlighted that a good improvement on the overall absorber properties is achieved by introducing inside the structure itself some cavities, an innovative solution. This design choice has led to a reduced weight of the mechanical structure and has shown a more progressive deformation during the impact.

The absorbers tested in this paper are all mainly made by honeycomb sandwich panels. Four different design configurations have been proposed and numerically tested in crash simulations (dynamic FEM analysis) by means of the explicit finite element code LS-DYNA in order to find out the best design configuration. Numerical simulations have shown the best configuration, in terms of technical performances and facility of realization, which has been

built up and experimentally validated, assessing a good correlation between the testing bench and the simulation results, through a drop-test performed at Politecnico of Milan (Italy).

An excellent correlation was found between the test and simulation results, because of an advanced quality in the solid discretization and a realistic material model (the Johnson-Cook model with a peculiar and original material characterization) for high-speed deformation material behaviour.

The innovative aspects of this activity are in the idea to use an appropriate alternation of sandwich panels with opportune cavities and the chosen modelling strategy for the materials behaviour. The experimental results obtained by means of the test bench are in very good agreement with the ones of the numerical crash simulation.

2. IMPACT ABSORBER CONFIGURATION

Four configurations have been considered and each absorber's structure is composed by six layers of sandwich panels each one made by one honeycomb and two skins attached on it. Core material is aluminium AA3003, while skin material is AA2024-T3. Skin thickness is 1 mm and core height is 32 mm, so that each panel height is 34 mm. Cores are made by several hexagonal prisms, having a thickness of about 0.2 mm and basis edge of 4 mm. On the top of each configuration there is a PVC block, to reach the minimum height, imposed by FSAE regulation.

2.1. Virtual Model

The geometry and mesh modeling of the virtual prototype have been realized using the BETA CAE ANSA, applying the following criteria:

(1) each Shell element has a QUAD geometry and an average area of 5 mm^2;
(2) each SOLID element has an hexa geometry, each solid element has been created by extruding a plane element of 5 mm^2, and by considering at least 3 solid elements in the thickness along the extrusion direction, in order to correctly model the bending behavior

In particular, below the Absober main elements and related mesh details are reported:

(1) Honeycomb panels (Skin-core-skin)-> external skins and internal core of the honeycomb panel have been modelled by SHELL elements, because of the not relevant thickness of the geometry;
(2) The Anti-intrusion plate and the PVC element and have been modeled with SOLID elements.

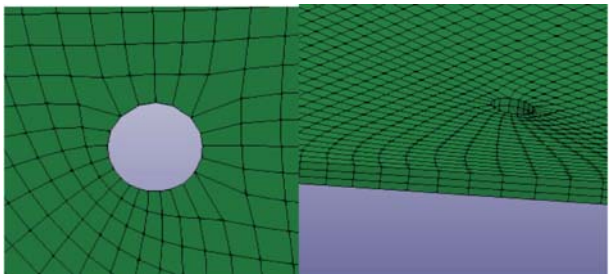

Figure 1. Mesh configuration.

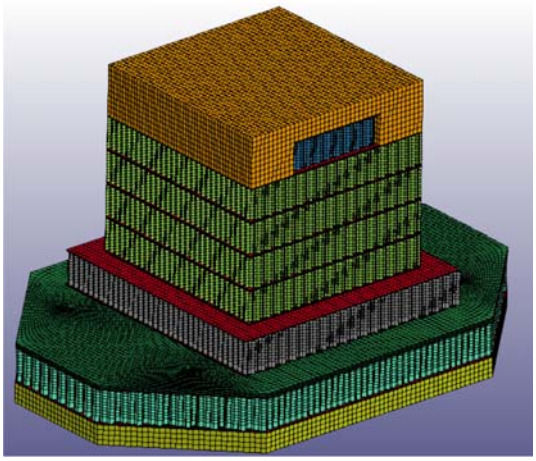

Figure 2. Virtual prototype.

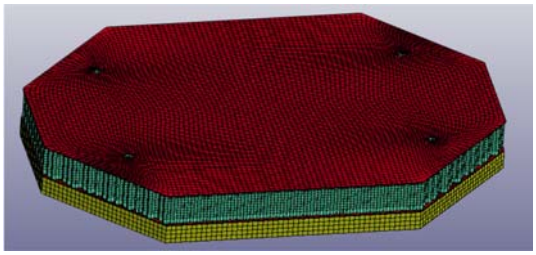

Figure 3. Absorber prototype.

2.1.1. First configuration: structure without any cavity

First panel perimeter measures 250 × 250 mm^2. Other four panels, having an area about 200 × 200 mm^2 are positioned on it, on the top is attached a 200 × 100 mm^2 panel, and at last there is the pvc block.

Structure's total height is 226 mm, while its weight is 2.67 Kg.

2.1.2. Second configuration: first cavity introduced

In the second configuration, differently from the first one, a

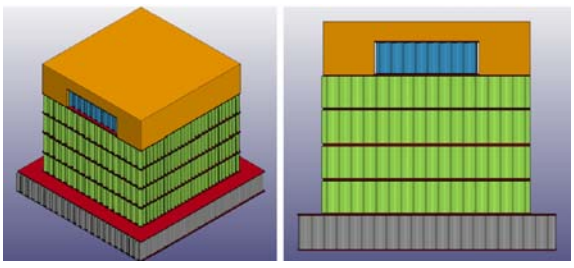

Figure 4. First configuration of the absorber structure.

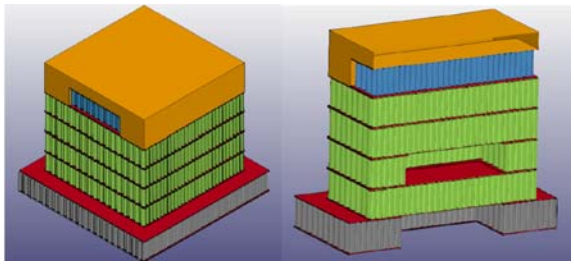

Figure 5. Second configuration of the absorber structure.

centred cavity in the first honeycomb panel has been introduced. This cavity measuring 125 × 125 mm, makes the impact attenuator lighter than the previous one, reaching 2.51 Kg.

2.1.3. Third configuration: two cavities introduced

In the third configuration the structure shows an added centred cavity on the third panel, of 115 × 115 mm. Weight's absorber becomes 2.37 Kg. The model alternates integral and centre-holed panels in the way that the overall structural integrity is preserved.

2.1.4. Fourth configuration: progressive variation of perimetral size

This attenuator has a pyramidal structure, composed by:

- First panel centred emptied, at the same of second and third configuration;
- Second panel having a 200 × 200 mm perimeter;
- Third panel measures 200 × 170 mm and has a centred cavity of 115 × 115 mm;
- Fourth panel has perimeter dimensions of 200 × 150 mm;

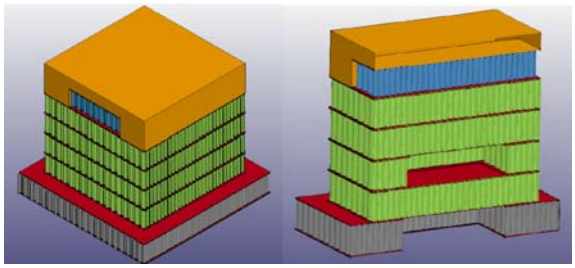

Figure 6. Third configuration of the absorber structure.

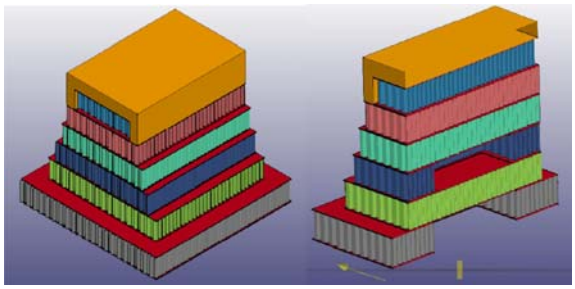

Figure 7. Fourth configuration of the absorber structure.

- Fifth panel has perimeter dimensions of 200 × 130 mm;
- Sixth panel has perimeter dimensions of 200 × 100 mm.

Structure's weight become 2.00 Kg.

On each configuration is attached the anti-intrusion plate in aluminium AA6082-T6, 4 mm thick. Behind this plate is bolted another honeycomb sandwich panel, having the same perimeter of the plate. Its upper skin is in carbon fibre, while the other skin is, like the other ones, in AA2024-T3.

The thickness of this added honeycomb panel is 50 mm, and its purpose is to simulate the vehicle's frame. The whole attenuator is elevated by a perimetral structure, allowing the free inflection of the anti-intrusion plate and of the last sandwich panel. Attenuator's height reaches 286 mm.

The finite element models have been created in BETA CAE ANSA. The accuracy of any impact simulation strongly depends on the mesh, the material models and the data used in the material models. Only hexa-elements for the solid ones have been used, while quad for the shells. These mesh elements have the greatest possible accuracy in the numerical simulations. As regards the material structural behaviour three different models have been considered:

- Cowper-Symonds (CS) for AA3003, AA6082-T6, carbon skin and PVC;
- Johnson-Cook (JC) for AA2024-T3;
- Rigid for the barrier and the end part of the structure.

The plastic-kinematic hardening model (CS) is a strain-rate dependent elastic-plastic model. It is suited to model isotropic and kinematic hardening plasticity. In this model, strain rate is accounted for using the Cowper-Symonds model which scales the yield stress by the strain rate dependent factor as shown below:

$$\sigma_y = 1 + \left(\frac{\dot{s}}{C}\right)^{\frac{1}{p}} \cdot \sigma_0 \qquad (1)$$

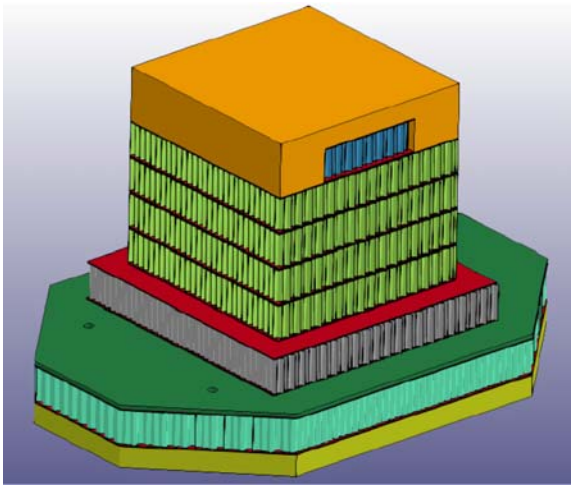

Figure 8. Entire absorber structure.

where σ_0 is the initial yield stress, $\dot{\varepsilon}$ is the strain rate; C and P are the Cowper-Symonds strain rate parameters.

Johnson and Cook model is a strain-rate and temperature-dependent (adiabatic assumption) visco-plastic material model (Johnson and Cook, 1983). This model is suitable for problems where strain rates vary on a large range, and temperature's change, due to plastic dissipation, causes material softening. The model is expressed in a multiplicative form of strain, strain-rate and temperature terms. The consequence of the multiplicative form is that the strain-hardening rate at, a certain strain, will increase when the strain rate increases.

The JC model represents the flow stress with an equation of the form:

$$\sigma = [A + B(\varepsilon_p)^n]\left[1 + c\ln\left(\frac{\dot{s}}{\dot{s}_0}\right)\right]\cdot\left[1 - \left(\frac{T - T_r}{T_m - T_r}\right)^m\right] \quad (2)$$

where σ is the effective stress, ε_P is the effective plastic strain, ε is the effective plastic strain rate (typically normalized to a strain rate of $\varepsilon_0 = 1.0\ s^{-1}$), A is the static yield limit, B the strain hardening modulus, C the strain rate coefficient, n the strain hardening exponent, m the thermal softening exponent, T_r is the room temperature, T_m the melting temperature and T the operating temperature.

Johnson and Cook expanded their basic model with the inclusion of a model for fracture based on cumulative damage; the LS-DYNA implementation of the JC constitutive model includes this addition model feature. The cumulative damage fracture is expressed as:

$$\varepsilon_f = \left[D_1 + D_2 e^{\left(D_3\frac{p}{q}\right)}\right]\cdot\left[1 + D_4\ln\left(\frac{\dot{s}_p}{\dot{s}_o}\right)\right]\cdot\left[1 + D_5\frac{T - T_r}{T_m - T_r}\right] \quad (3)$$

where ε_f is the effective plastic strain, D_1, D_2, D_3, D_4 and D_5 are five constants, p is the hydrostatic tension and q the Von Mises equivalent stress. So the JC fracture model is similar in form to the yield strength model, with three terms combined in a multiplicative manner to include the effects of stress triaxiality, strain rate and local heating, respectively.

Additionally, the elastic parameters are required in all these models.

The calibrated input parameters used in the present analysis are given in Table 1.

For the CS models, the values p and q haven't been considered, that is to say the independence from strain rate.

The above parameters in Table 1 represent an original characterization of the material not present in literature. They have been numerically validated in LS-DYNA by means of "virtual" replication of traction, bending and torsion tests, to simulate high-speed stress propagation and high-speed fracture modes. By numerical simulation the stress-strain curves have been computed and the JC parameters have been taken out by fitting the obtained curve through JC equations.

Table 1. JC parameters of AA2024-T3. (Kay, 2003)

A [MPa]	B [MPa]	n	C	m
265	426	0.34	0.015	1.0
T_r [K]	T_m [K]	C_p [J/Kg K]	ρ [Kg/m^3]	E [MPa]
294	775	875	2770	72000

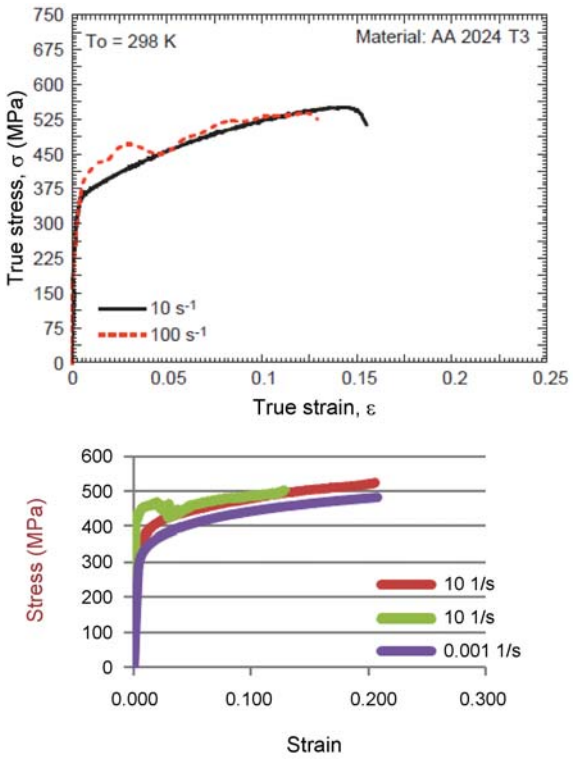

Figure 9. Stress-strain values comparison between curves available in literature and simulations outcome.

When the pressure generated by shock wave propagation exceeds the material strength by several orders of magnitude, the early stages of material response can be regarded as hydrodynamic; strength effect appears in the

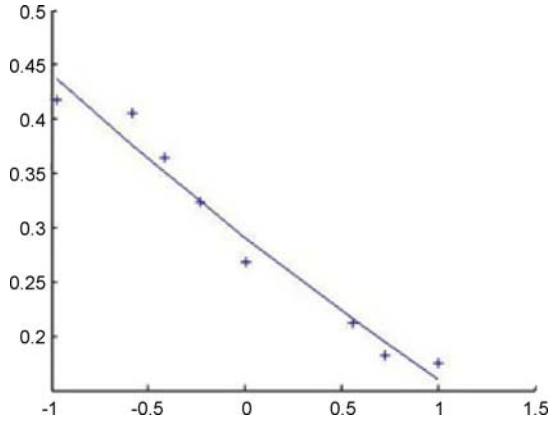

Figure 10. Fracture model parameters values comparison between literature results and simulations outcome.

Table 2. Fracture model parameters.

	D_1	D_2	D_3
Parameters obtained by best fitting of fracture data from simulation analysis	0.138	0.124	− 1.560
Proposed parameters	0.130	0.130	− 1.500
variation %	6 .1 %	4.6 %	4.0 %

late stages of the event.

Therefore, it is assumed for both metal materials that volumetric behaviour is described by the Mie- Grüneisen equation of state (EOS) model:

$$P = \frac{\rho_0 c_0^2 \mu \left[1 + \left(1 - \frac{\gamma_0}{2}\right)\mu - \frac{a}{2}\mu^2\right]}{\left[1 - (S_1 - 1)\mu - S_2 \frac{\mu^2}{\mu + 1} - S_2 \frac{\mu^3}{(\mu + 1)^2}\right]} + (\gamma_0 + a\mu)e \quad (4)$$

in which γ_0 is the Grüneisen coefficient, c_0 the velocity of propagation of sound, s is the shock wave velocity parameter and it defines the linear relationship between the shock velocity and the particle velocity. The values of these parameters used in this analysis are given in Table 3.

Surface-to-surface type contact interface has been used for the contact between the barrier and the impact attenuator. This type has been selected so that impact attenuator's internal nodes could be in contact with the rigid barrier during the simulation procedure.

Contacts tied-surface-to-surface have been defined between PVC and skins, anti-intrusion plate and rear structure, skins; while between core and skins a tied-nodes-to-surface type contact has been used. To consider interactions between the various parts, a single-surface contact has been considered on the set of all the parts of impact attenuator.

Finally, to start simulation, we needed to define boundary conditions and initial conditions: an INITIAL-VELOCITY-GENERATION of 7 m/s has been set on the barrier and the rear structure of the impact attenuator has been constrained in all degrees of freedom.

Simulated results obtained are shown in Figure 11, 12, 13, 14.

In Table 4 the results of the main characteristics to consider in the analysis of each configuration are shown.

The rate SEA has been used in order to make a better comparison between the different configurations. It is defined as:

Table 3. Input parameters for the Mie-Gruneisen EOS model (Plassard *et al.*, 2011).

Y_0	c_0 [m/s]	S_1	S_2	S_3
2.0	5536	1.338	0.0	0.0

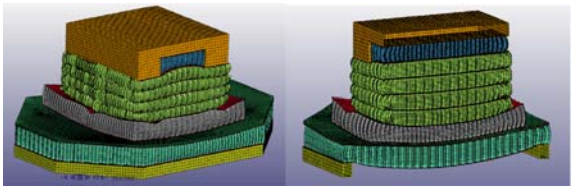

Figure 11. Simulation results of configuration 1.

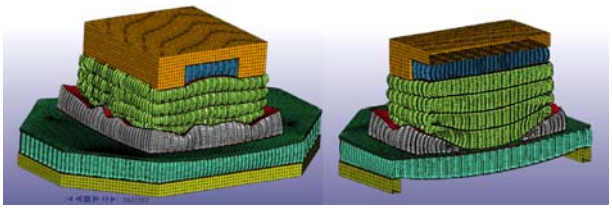

Figure 12. Simulation results of configuration 2.

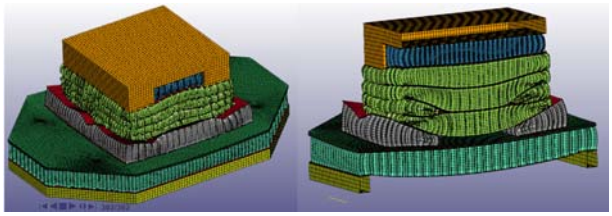

Figure 13. Simulation results of configuration 3.

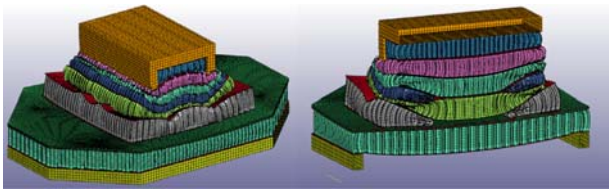

Figure 14. Simulation results of configuration 4.

$$\text{SEA} = \frac{Ea}{M}\left[\frac{J}{Kg}\right] \quad (5)$$

It expresses the amount of absorbed energy compared to the absorber's mass, therefore it allows to understand which structure absorbs more energy for a given weight, or to understand what structure is lighter for a given absorbed energy value.

As shown from Table 4 switching from configuration 1 to 4 the values of inflection, maximum and average deceleration decrease.

3. FROM SIMULATION ENVIRONMENT TO THE REAL TESTING

3.1. Regulatory Constraints and Test Design

The competition's normative establishes some geometric limits and technical performances on the crash box.

As concerns geometric limits, minimum dimensions are imposed: the absorber must be long at least 200 mm, while

Table 4. Reference parameters' values of the analysis.

	Mass structure (M) [Kg]	Kinetic energy absorbed (Ea) [J]	SEA [J/Kg]	anti-intrusion plate's inflection [mm]	Maximum deceleration [g]	Average deceleration [g]
Config.1	5.43	7740	1425.41	21.5	31.97	18.91
Config.2	5.27	7740	1468.69	16.1	28.61	17.30
Config.3	5.13	7740	1508.77	12.9	26.97	16.48
Config.4	4.79	7740	1615.86	12.3	23.01	14.52

transversal dimensions must be at least 200 × 100 mm. Moreover, it has been placed in front of the frame's bulkhead at a distance of 200 mm from it, so that it should not penetrate the bulkhead during a collision.

If the absorber is made by foam or by honeycomb, it must be attached to an anti-intrusion plate, having thickness of 4 mm (if aluminium) or 1.5 (if steel). This plate should have the same dimensions of the bulkhead and has to be linked to it by welding or by bolting (4 × M8).

As concerns technical performances, the crash box has to decelerate the vehicle so that it moves at 7 m/s along the longitudinal direction, parallel to the bigger absorber's axis.

Consequently, the absorbed energy during the impact is about 7350 J. Indeed, for a vehicle going on straight trajectory, in a constant velocity condition, the main contribution to the total energy value is given by kinetic energy.

The vehicle's average deceleration must be lower than 20 g, and the maximum deceleration value lower than 40 g. Experimental acceleration datasets have to be filtered by CFC (channel filter class) at 100 Hz or by a Butterworth low-pass filter (−3 dB at 100 Hz).

Moreover, a limit on the anti-intrusion plate's inflection is imposed: it must be lower than 25.4 mm.

3.2. Physical Prototype

It has been decided to test the third attenuator's configuration, in order to have a trade-off between good technical performances and an easy production method.

At first honeycomb sandwich panels have been prepared to be cut. After drawing the cut frame on panels surfaces, they have been cut by flex.

PVC block has been composed by three components: one having a perimeter of about 200 × 200 mm to completely cover intermediate perimeters' panels below, and other two blocks 50 × 50 × 200 mm put on each side of the last panel.

Then anti-intrusion plate has been cut, and on it four holes M8 have been done by an axial drill. In order to prepare aluminium panel's surfaces to be pasted, they have been carefully cleaned by acetone. This procedure doesn't allow impurities compromising a good pasting between skins' panels. After cleaned contact's surfaces, they have been abraded in order to remove upper oxidized material's

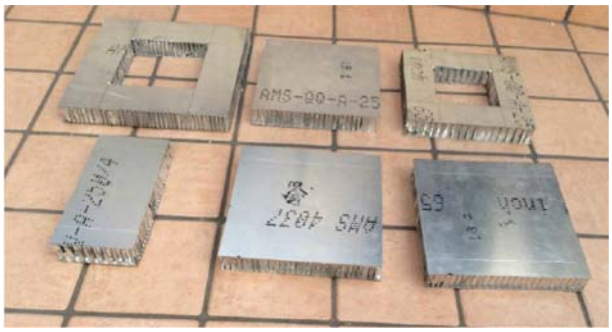

Figure 15. Sandwich honeycomb panels.

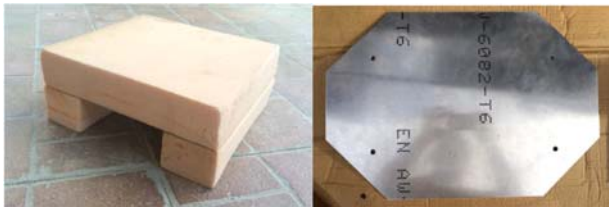

Figure 16. PVC block (on the left) and anti-intrusion plate (on the right).

layer and to increase roughness' surface: a good roughness allows a better affinity between aluminium and resin.

Then all panels and the plate have been pasted by an epoxy resin, LOCTITE® EA 9466™.

Behind the anti-intrusion plate a structure, simulating the

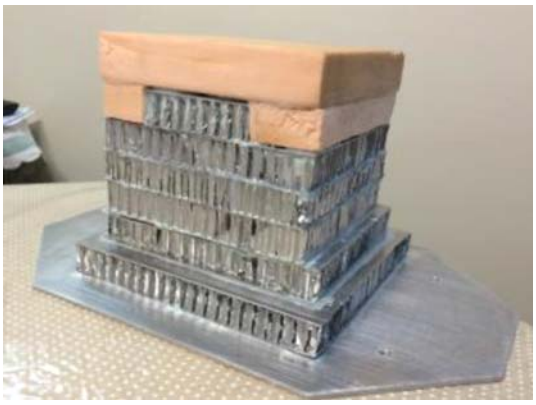

Figure 17. Attenuator's structure with anti-intrusion plate.

Figure 18. Structure behind the anti-intrusion plate.

vehicle's frame, has been bolted.

This structure has the same plate's contour, since it is made by honeycomb sandwich panel and it is upper covered by four carbon fiber layers, in order to reproduce the same material of vehicle's frame.

Carbon layers' fibers have been oriented symmetrically 0-90-90-0 degree.

Around this structure there is a perimetral flexed honeycomb panel, measuring 1110 × 50 × 50 mm, pasted on it by L links.

Finally the whole structure, showed in next figure, reaches an height of 286 mm and it weighs 5.07 Kg.

3.3. Experimental Setup

In order to verify the reglementary design constraints and to experimentally validate modelling results, the impact attenuator has been tested at Politecnico of Milan (Italy). This test has been made by using a drop tower by dropping a mass of 300 kg from an height of 2.6 m, in order to achieve a final impact velocity of 7 m/s.

Figure 21 shows the setup of impact test and Figure 23 shows the deformed attenuator after the drop test.

Figure 19. Elements behind the anti-intrusion plate.

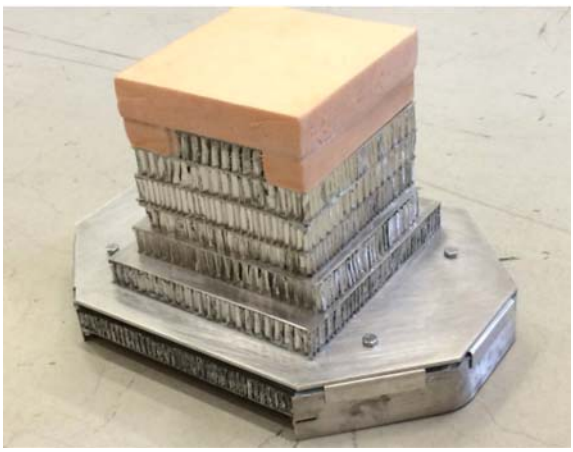

Figure 20. Whole attenuator's structure.

Two accelerometers put on the dropping mass have measured acceleration's values. The signals so obtained have been filtered by CFC (channel filter class) at 100 Hz. From acceleration's signal, by integration, we can have velocity and displacement diagrams, from which it is possible to derive the absorbed energy and force diagrams, as represented in Figure 23.

Moreover, anti-intrusion plate's inflection has been measured as a distance between the upper plate's extremity and a rigid undeformed bar laid on it, by a caliber, as shown in Figure 24.

Average and maximum deceleration's values are respectively 18.1 g and 27.75 g, while anti-intrusion plate's inflection measured is 12.0 mm.

Figure 21. Phase pre-crash.

Figure 22. Phase post-crash.

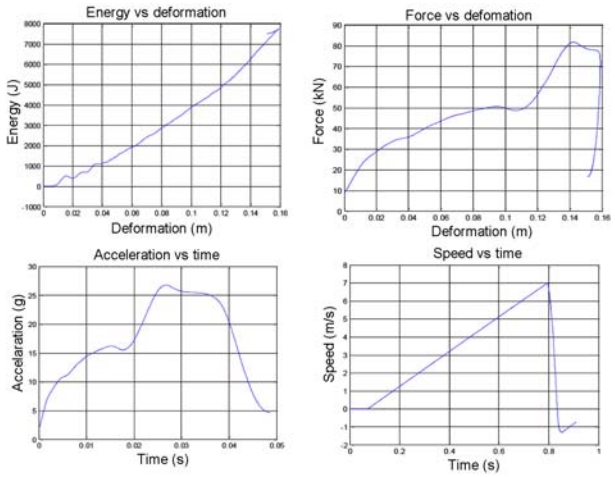

Figure 23. Acquired signals (force, deformation, acceleration and velocity) and derived energy quantity.

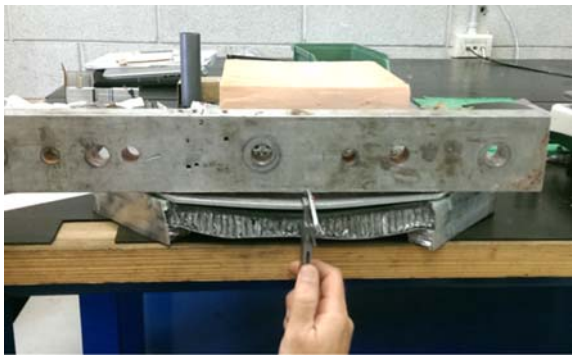

Figure 24. Whole attenuator's structure.

Table 4. Reference parameters values.

	Experimental test	Dynamic Simulation	Variation (%)
Height variation $\left(\frac{l_f - l_i}{l_i} \cdot 100\right)$	46.1 %	40.6 %	-
Velocity	7.01 m/s	7 m/s	-
Absorbed energy	7740 J	7740 J	-
Average deceleration	18.10 g	16.48 g	8.9 %
Maximum deceleration	27.75 g[(1)]	26.97 g	2.8 %
Anti-intrusion plate's inflection	12.0 mm	12.9 mm	7.5 %

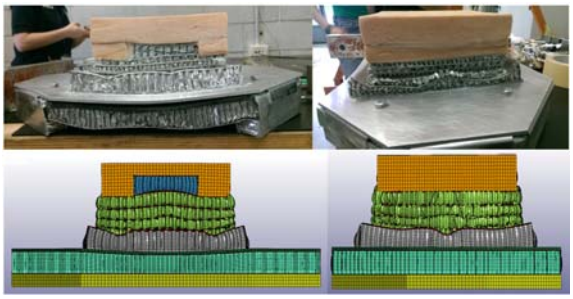

Figure 25. Frontal and lateral view of post-crash results.

4. RESULTS AND COMPARISON

In Table 4 the references parameters of the analysis, deriving from experimental test and simulation in LS-DYNA, are reported.

Variation between datas deriving from the simulation and experimental test are lower than 10 %, so FEM

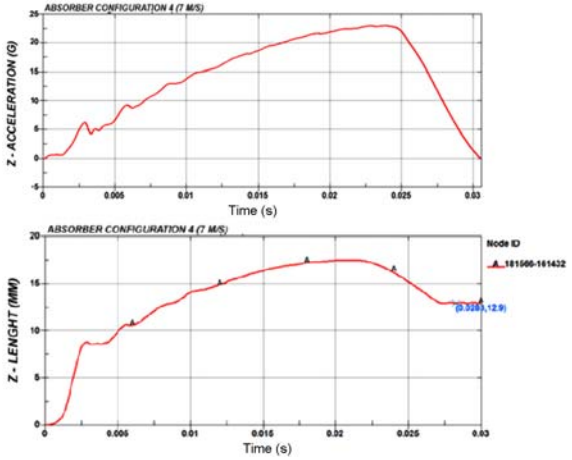

Figure 26. Comparison between simulation results and testing data.

analysis' results can be considered acceptable.

In the following pictures (Figure 25 and 26) real structure's deformation and FEM model's deformation are compared, highlighting a good agreement between the simulated results and acquired data.

5. CONCLUSION

In this paper the design of an innovative impact attenuator, made up of honeycomb sandwich panels realized by using different aluminium alloys, to be mounted on a Formula SAE car to get the optimal crash energy management, to maximize the absorbed energy and to optimize the geometry has been presented.

The main focus has been on component geometry optimization to reach the best achievable performances in term of structural integrity, deformation capability, light weighted characteristic and compliance to FSAE safety requirements. The outcome of this study has highlighted that a good improvement on the overall absorber properties is achieved by introducing an innovative solution: some cavities inside the structure. This design choice has led to a reduced weight of the mechanical structure and has shown a more progressive deformation during the impact.

Four different design configurations of the crash box have been proposed and numerically tested in crash simulations by the explicit finite element code LS-DYNA, in order to find out the best configuration. This last that has built up and experimentally validated through a drop-test performed at Politecnico of Milan (Italy).

The crash-tests have been performed measuring the load-shortening diagram, the deceleration and the energy absorbed by the structure.

Thanks to an advanced quality in the solid discretization and a realistic material model (the Johnson-Cook model with a peculiar and original material characterization) for high-speed deformation material behaviour, an excellent correlation was found between the experimental test and simulation results. This allows to validate the optimization study done before the drop test.

ACKNOWLEDGEMENT–The authors would like to thank Eng. Andrea Milanese of the Politecnico of Milan for his support in the experimental activity and the Formula Sae team of University of Naples for the support in the prototypes realization.

REFERENCES

2017-18 Formula SAE® Rules (2017). https://www.fsaeonline.com/content/2017-18-FSAE-Rules-091317.pdf

Ahmadisoleymani, S. S. and Missoum, S. (2017). Risk prediction of traumatic brain injury from car accidents. *ASME 2017 Int. Mechanical Engineering Cong. and Expo.* American Society of Mechanical Engineers Digital Collection.

Belingardi, G. and Obradovic, J. (2010). Design of the impact attenuator for a formula student racing car: numerical simulation of the impact crash test. *J. Serbian Society for Computational Mechanics* **4**, **1**, 52–65.

Boria, S. (2016). Numerical and experimental analysis of an impact attenuator in sandwich material for racing application, *Int. J. Science, Engineering and Technology Research*, **5**, **6**, 1909–1913.

D'Agostino, L., Bertocchi, L., Splendi, L., Strozzi, A. and Moruzzi, P. (2013). Optimization methodology for innovative automotive crash absorbers. *ASME 2013 Int. Mechanical Engineering Cong. and Expo*. American Society of Mechanical Engineers Digital Collection.

Kay, G. (2003). Failure modeling of titanium 6al-4v and aluminium 2024-t3 with the johnson-cook material model. *U.S. Department of Transportation Federal Aviation Administration.*

Johnson, G. R. and Cook, W. H. (1983). A constitutive model and data for metals subjected to large strains, high strain rates and high temperatures. *Proc. 7th Int. Symp. Ballistics*, Hague, Netherlands, 541–547.

Ma, D. and Lankarani, H. M. (1997). A multibody/finite element analysis approach for modeling of crash dynamic responses. *J. Mechanical Design* **119**, **3**, 382–387.

Plassard, P., Mespoulet, J. and Hereil, P. (2011). Hypervelocity impact of aluminium sphere against aluminium plate: experiment and LS-DYNA correlation. *Proc. 8th European LS-DYNA Users Conf.*, Strasbourg, France.

Potabatti, N. S. (2016). Design and physical testing of impact attenuator for formula SAE racecar, *Int. J. Science, Engineering and Technology Research* **5**, **1**, 357–360.

Ruan, D., Lu, G., Wang, B. and Yu, T. X. (2003). In-plane dynamic crushing of honeycombs—a finite element study, *Int. J. Impact Eng*., **28**, **2**, 161–182.

Wu, E. and Jiang, W. S. (1997). Axial crush of metallic honeycombs, *Int. J. Impact Eng*., **19**, **5-6**, 439–456.

Yamashita, M. and Gotoh, M. (2005). Impact behaviour of honeycomb structures with various cell specifications—numerical simulation and experiment, *Int. J. Impact Eng.* **32**, **1-4**, 618–630.

Zhao, H. and Gary, G. (1998), Crushing behaviour of aluminium honeycombs under impact loading, *Int. J. Impact Eng.*, **21**, **10**, 827–836.

Zhou, C., Jiang, L., Tian, K., Bi, X. and Wang, B. (2017). Origami crash boxes subjected to dynamic oblique loading. *J. Appl. Mech*. **84**, **9**, 091006-1-091006-11.